

碳纤维复合材料激光热-机械剥蚀机制研究

梁晗^{1,2,3}, 赵树森^{1,3*}, 姜璐^{1,2,3}, 邹晨¹, 许杰¹, 张志研^{1,3}, 林学春^{1,2,3}¹中国科学院半导体研究所全固态光源实验室, 北京 100083;²中国科学院大学材料科学与光电技术学院, 北京 100049;³北京市全固态激光先进制造工程技术研究中心, 北京 100083

摘要 针对航空复合材料挖补修复工艺对损伤区高效高质量去除的需求,研究了碳纤维复合材料纳秒脉冲激光剥蚀机理、工艺优化和缺陷控制方法,基于各向异性传热原理研究了激光扫描角度对材料去除率的影响规律,探索了激光扫描速度和填充间距对非匀质材料的热-机械剥蚀的影响机制。结果表明:碳纤维复合材料显著的各向异性传热使得去除深度随激光扫描角度的增大而减小,激光扫描角度为 0° 时去除深度为 $220\ \mu\text{m}$,激光扫描角度为 90° 时去除深度为 $150\ \mu\text{m}$;由于热-机械剥蚀的混合作用,两个方向上的光斑搭接率存在临界值,在该临界值处材料去除效率出现峰值。进行了 18 层的阶梯形去除,精度控制在 $\pm 20\ \mu\text{m}$ 。通过实验测试与数据分析,优化了碳纤维复合材料逐层精细剥蚀扫描策略与工艺方案,为碳纤维激光精细制造提供了参考。

关键词 激光技术; 脉冲激光; 碳纤维复合材料; 挖补修复; 热-机械剥蚀; 逐层去除

中图分类号 TN219

文献标志码 A

DOI: 10.3788/CJL202249.1002405

1 引言

碳纤维复合材料(CFRP)凭借其比强度高、比模量大的优势,被广泛应用于航天航空、体育、医疗、交通等领域。以波音 787 为例,复合材料用量(质量占比)已经达到 50% ^[1]。恶劣环境中长时间服役使得飞机上的复合材料结构易受损伤,复合材料结构修补是航空装备维护的一项重要工作^[2]。复合材料挖补的关键环节是损伤区的小角度、高质量去除,挖补角度通常为 $2^\circ\sim 6^\circ$,机械加工难度大,目前主要依靠人工打磨,效率低且可控性差。激光精密加工具有高精度、高效率、高可控性优势,适用于包括 CFRP 在内的各类难加工材料,在激光切割、钻孔、焊接、清洗、刻蚀等领域表现优异^[3-9]。

采用激光逐层去除 CFRP 材料损伤区域是激光精密加工的一个新兴应用,目前相关研究主要集中在两方面:一是激光作用的热效应,二是工艺参数优化。Fujita 等^[10-13]研究发现,采用 $355\ \text{nm}$

短波长激光能够有效减小热效应,但加工效率较低; $1064\ \text{nm}$ 纳秒脉冲激光加工效率高,但出现氧化分层、热影响区(HAZ)较大等问题。Fischer 等^[14]采用短波长、窄脉宽的激光器进行了 CFRP 的逐层去除加工,得到了较小的热影响区,保证了激光加工后碳纤维的完整性。Schmutzler 等^[15]采用 $1064\ \text{nm}$ 纳秒脉冲激光对 CFRP 粘接表面进行了激光处理,发现适当的热效应使碳纤维表面发生氧化并生成一些特定官能团后,有利于提高碳纤维与黏结剂的结合强度。Genna 等^[16-17]通过 $1064\ \text{nm}$ 纳秒激光对 CFRP 待粘接面进行了表面预处理,发现黏接时新的树脂基体与激光作用后暴露出的碳纤维之间的接触能够增大接触面积,从而增强结合性能,经测试剪切强度提高了两倍。以上研究集中于不同波长激光作用 CFRP 材料时的热效应,结果表明,相对 $355\ \text{nm}$ 紫外激光, $1064\ \text{nm}$ 激光加工 CFRP 时热影响区较大,但碳纤维表面发生高温氧化,有助于提高基材表面与补片之间的粘接强度。

收稿日期: 2021-12-01; 修回日期: 2021-12-23; 录用日期: 2022-01-25

基金项目: 国家自然科学基金(U2033211)

通信作者: *zhaoshusen@semi.ac.cn

工艺规律探索方面,胡俊等^[18-19]研究了碳纤维复合材料激光去除工艺规律,发现提高扫描速度、增大填充间距会减小去除深度,但去除效率不是单调变化的。Loutas 等^[20-22]研究发现,填充间距为 100 μm 时,提高重复频率会增大热影响区,降低剪切强度;填充间距为 250 μm 时,提高重复频率会减小热影响区,剪切强度呈现上升趋势。在 30 kHz 的重复频率下,扫描方向垂直于碳纤维时的热影响区大于扫描方向平行于碳纤维时的热影响区,而在 80 kHz 的重复频率下,规律是相反的。Holder 等^[23]在使用纳秒红外激光器进行激光挖补 CFRP 时,通过去除深度在线检测与反馈控制技术,实现了去除深度误差小于 10 μm ,去除效率达到 432 mm^3/min 。Ledesma 等^[24]研究了不同激光参数处理后 CFRP 的断裂过程和失效模式。上述关于工艺的研究主要集中于工艺参数优化,并发现不同参数下存在不同的激光烧蚀机制,对加工效果产生显著影响。

综上,CFRP 材料结构与组分热物性差异导致 CFRP 复合材料的激光去除比金属材料具有更为复杂的物理过程^[25-26]。已有的文献报道主要集中于 CFRP 材料激光去除中热过程的探讨,以及由此带来的表面状态演化规律,但是对于 CFRP 非匀质材料激光去除过程的热-机械剥蚀工艺规律关注较少。本文基于 1064 nm 纳秒脉冲激光研究了工艺参数对去除效率和质量的影响规律以及优化方法,基于各向异性传热机理研究了激光扫描方向对材料去除率的影响规律,探索了光斑搭接率对非匀质材料的热-机械剥蚀影响的规律与物理机制,获得了 CFRP 层板 18 层阶梯形激光去除结果,并讨论了激光离焦状态对去除效果的影响。

2 材料、设备和实验设计

2.1 材料

所用材料为多向和单向铺层的碳纤维复合层板,其中单向铺层碳纤维复合层板为 T300 级碳纤维,树脂基体为双酚 A 型环氧树脂,采用真空袋压成型工艺,在 120 $^{\circ}\text{C}$ 下固化 90 min,真空压强为 8×10^4 Pa。碳纤维板尺寸为 100 mm \times 100 mm \times 2.5 mm,铺层方向为单向铺层,表面无编织层,详细物性参数如表 1 所示。多向铺层碳纤维复合层板为 T700 级碳纤维,树脂基体为双马来酰亚胺树脂,碳纤维层单层厚度为 125 μm ,铺层方向为 $[90^{\circ}/-45^{\circ}/0^{\circ}/45^{\circ}/90^{\circ}]_s$,其中角标 s 代表铺层关于

中面对称。

表 1 CFRP 各组分物性参数

Table 1 Physical parameters of CFRP components

| Parameter | Matrix | Carbon fiber (radial) | Carbon fiber (axial) |
|---|--------|-----------------------|----------------------|
| Density / ($\text{kg} \cdot \text{m}^{-3}$) | 1160 | 1850 | 1850 |
| Evaporation temperature / K | 700 | 4000 | 4000 |
| Heat capacity / [$\text{J} \cdot (\text{kg} \cdot \text{K})^{-1}$] | 1200 | 710 | 710 |
| Heat conductivity / [$\text{W} \cdot (\text{m} \cdot \text{K})^{-1}$] | 0.2 | 5 | 50 |

2.2 设备

所用激光器为 IPG 公司生产的纳秒脉冲激光器,波长为 1064 nm,最大功率为 30 W,脉冲宽度为 4~200 ns,脉冲重复频率为 1~1000 kHz,本实验设置激光脉宽 t 为 200 ns,重复频率 f 为 50 kHz。采用 SCANLAB 公司生产的 SCANcube10 振镜实现二维加工,场镜焦距为 160 mm,该场镜下焦点处圆形光斑半径 r 约为 30 μm 。最大功率下单脉冲能量为 0.6 mJ,峰值功率密度为 1.06×10^8 W/cm^2 。去除深度数据和表面轮廓形貌通过上海光学仪器一厂生产的 SRA-2 轮廓仪测量获得,材料表面宏观和微观形貌通过上海光学仪器一厂生产的 XYH-3A 体视显微镜、上海永亨光学仪器制造有限公司生产的 9XB-PC 光学显微镜以及蔡司公司生产的 EVO[®]18 扫描电子显微镜观测获得。

2.3 实验设计

激光作用在 30 mm \times 30 mm 的正方形区域上,扫描路径为图 1 所示的“弓”字形,其中实线代表开光状态,虚线代表关光状态。测试去除深度 h 随功率 P 、扫描速度 v 、填充间距 d ,扫描角度 θ 和离焦距离 l 的变化规律,同时计算出对应的去除效率 (MRR, Material Removal Rate) 随加工参数的变化规律,其中扫描角度 θ 为图 1 所示的扫描路径与碳纤维的夹角,扫描速度和填充间距分别决定了沿扫描路径的光斑搭接率 α_A 和垂直于扫描路径的光斑搭接率 α_B :

$$\alpha_A = 1 - \frac{v}{2rf}, \quad (1)$$

$$\alpha_B = 1 - \frac{d}{2r}. \quad (2)$$

去除效率 R_{MR} 为

$$R_{\text{MR}} = h d v. \quad (3)$$

详细实验参数如表 2 所示。对于 D 组参数,

基于原有光斑尺寸,光斑搭接率 α_B 为 70% 时,填充间距为 $18 \mu\text{m}$,烧蚀严重,不能获得有效数据,为了获得光斑搭接率 α_B 对热-机械剥蚀效果的影响规律,调节离焦距离,使样品表面激光光斑半径 r 约为 $50 \mu\text{m}$ 。

为保证数据可靠性,采用每组参数扫描三次后测量去除深度的方式,并且在多个样品上进行重复实验,每组数据由 10 组数据求均值得出。通过扫描电镜观察不同参数作用后的 CFRP 表面形貌,判断去除质量并分析作用机制。

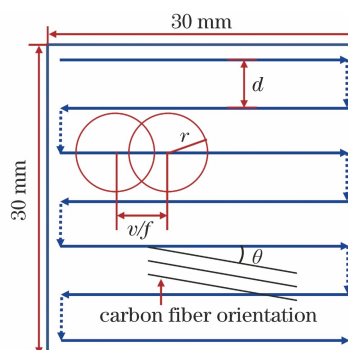


图 1 扫描路径示意图

Fig. 1 Schematic of scanning path

表 2 实验参数

Table 2 Experimental parameters

| Label | Power P /W | Scanning speed v /(mm/s) | Scanning angle θ /(°) | Hatch distance d / μm |
|-------|--|--|------------------------------|--|
| A | 1.8/3.6/6.0/9.0/12.0/15.0/ 18.0/21.0/24.0/27.0/30.0 | 460 | 0 | 40 |
| B | 30 | 400/700 | 0/15/30/45/60/75/90 | 40 |
| C | 30 | 100/200/300/400/500/600/ 700/800/900/1000/1100/ 1200/1300/1400/1500/ 1600/2600/2800/3000/3200/ 3400/3600/3800/4000 | 0 | 40 |
| D | 30 | 500 | 0/90 | 30/40/50/60/70/80/90/ 100/110/120/130/140/ 150/160/170/180 |
| E | 30 | 380 | 0 | 40 |

3 实验结果与讨论

3.1 峰值功率密度对去除效果的影响

图 2 为采用 A 组参数测得的去除深度随峰值功率密度的变化曲线,二者呈线性关系。CFRP 中环氧树脂基体对 1064 nm 波长激光的透过率约为 80% ^[14],红外激光加工 CFRP 时大部分激光透过表层树脂直接作用到碳纤维上,使其升温并发生氧化气化,同时在热传导的作用下,碳纤维周围的环氧树脂被加热发生烧蚀气化。激光平均功率 1.6 W 时,峰值功率密度为 $6.35 \times 10^6 \text{ W/cm}^2$,激光透过表层树脂加热碳纤维,产生的热量不足以直接烧蚀气化碳纤维,而是通过热传导加热烧蚀掉表层树脂和碳纤维之间的部分树脂,使碳纤维与表层树脂分离,如图 3(a)所示。激光平均功率为 3.6 W ,峰值功率密度增大到 $1.27 \times 10^7 \text{ W/cm}^2$ 后,热传导使得表层树脂能够完全烧蚀气化,但仍不足以直接烧蚀气化碳纤维,此时部分碳纤维被氧化,变得疏松多孔,同时表层碳纤维之间的树脂发生热解气化,生成气体的反冲压力的作用使得氧化后疏松多孔的碳纤维被破

坏,如图 3(b)所示,纤维丝断裂并卷曲翘起。激光平均功率为 30 W ,峰值功率密度达到 $1.06 \times 10^8 \text{ W/cm}^2$ 时,脉冲激光作用产生的温度足以直接烧蚀气化碳纤维。为了清楚观测碳纤维断口形态,在 A 组参数基础上,填充间距设置为 $300 \mu\text{m}$,表面及碳纤维断口形貌如图 3(c)、(d)所示,其中图 3(d)为图 3(c)扫描轨迹上的局部放大,可以看出,碳纤维呈现规则的椭球状断口形貌。

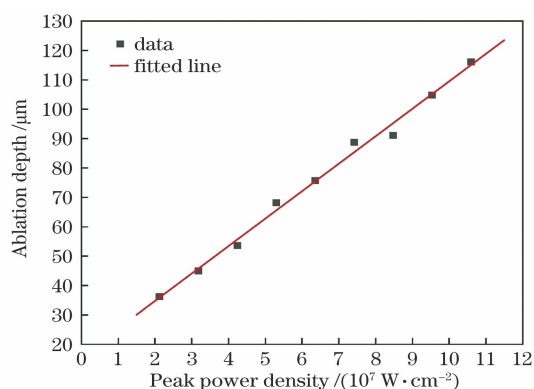


图 2 峰值功率密度对烧蚀深度的影响规律

Fig. 2 Influence of peak power density on ablation depth

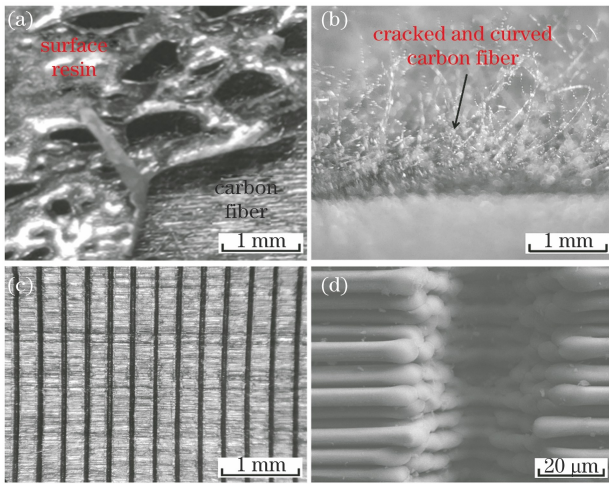


图 3 不同峰值功率密度下 CFRP 表面烧蚀形貌。
 (a) $6.35 \times 10^6 \text{ W/cm}^2$; (b) $1.27 \times 10^7 \text{ W/cm}^2$;
 (c) $1.06 \times 10^8 \text{ W/cm}^2$; (d) 图 3(c) 凹槽处的微观形貌
 Fig. 3 Ablation morphologies of CFRP surface under
 different peak power densities. (a) $6.35 \times 10^6 \text{ W/cm}^2$;
 (b) $1.27 \times 10^7 \text{ W/cm}^2$; (c) $1.06 \times 10^8 \text{ W/cm}^2$;
 (d) microscopic morphology of groove in Fig. 3 (c)

3.2 基于各向异性传热的扫描角度优化

扫描角度即扫描路径与碳纤维方向的夹角, 图 4 为根据 B 组参数测试的扫描角度对去除深度的影响规律, 去除深度随扫描角度的增大而减小, 这是由碳纤维各向异性传热导致的。激光作用在 CFRP 上时通过热传导加热周围区域, 对后续去除过程起到了预热作用。碳纤维轴向热导率为径向热导率的 10 倍, 脉冲作用后会形成椭圆形的温度场,

其长轴沿碳纤维轴向, 预热作用较强, 短轴沿碳纤维径向, 预热作用较弱。扫描角度为 0° , 即激光沿碳纤维轴向扫描时, 激光扫描路径上的预热作用强, 整体温度更高, 去除深度更大, 随着扫描角度的增大, 激光扫描路径上的预热作用减弱, 整体温度降低, 去除深度减小。对比 400 mm/s 和 700 mm/s 扫描速度下去除深度随扫描角度的变化趋势发现, 低扫描速度时, 扫描角度的影响更大, 这是因为低扫描速度时预热作用导致的热积累的影响更显著。如图 5 所示, 对比 0° 平行扫描和 90° 垂直扫描时的表面形貌发现, 90° 扫描时底层碳纤维烧蚀断裂更为严重, 会影响修补处的力学性能。综合不同扫描角度下的去除效率和去除质量, 分析认为, 对于实际工艺应用, 采取措施保持 0° 的扫描角度可以有效提高加工效率和加工质量。

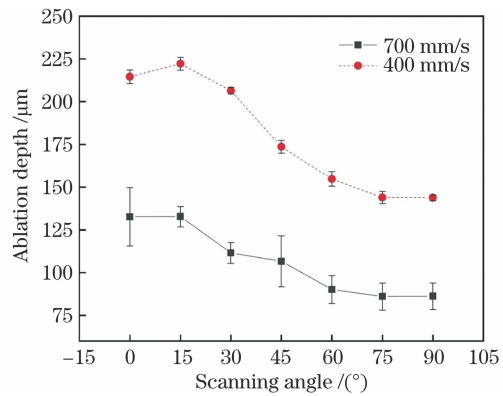


图 4 扫描角度对去除深度的影响规律
 Fig. 4 Influence of scanning angle on ablation depth

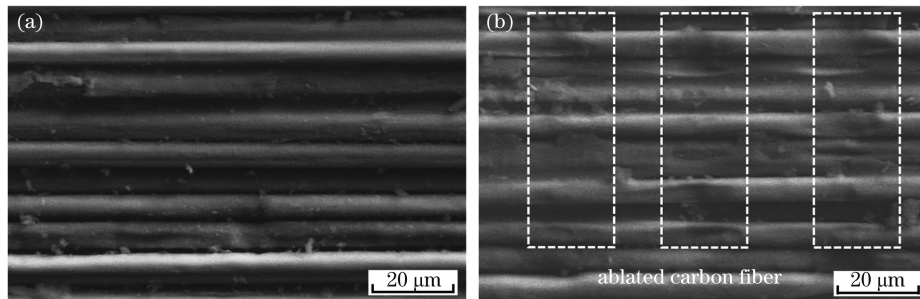


图 5 CFRP 表面形貌对比。(a) 0° 平行扫描; (b) 90° 垂直扫描
 Fig. 5 Surface topographies of CFRP. (a) 0° parallel scanning; (b) 90° vertical scanning

3.3 光斑搭接率与热-机械剥蚀作用的关系

光斑搭接率包括沿扫描路径的光斑搭接率 α_A 和垂直于扫描路径的光斑搭接率 α_B , 由于光斑直径和脉冲重复频率固定, 因此扫描速度和填充间距能够分别体现 α_A 和 α_B 的影响规律。图 6(a) 所示为扫描速度为 100 mm/s 时, 相邻脉冲之间的距离为 $2 \mu\text{m}$ 的激光烧蚀表面形貌, 此时光斑搭接率 α_A 为 97% , 热积累严重, 温度较高, 发生剧烈燃烧, 表面碳

纤维周围的树脂被烧蚀气化去除, 而燃烧时的热量不足以气化碳纤维, 因此在表面留下了一层氧化严重的松散碳纤维, 可以被轻易剥除, 表面形貌破坏严重。图 6(b) 为 400 mm/s 的扫描速度下的表面形貌, 此时相邻脉冲之间的距离为 $8 \mu\text{m}$, 光斑搭接率 α_A 为 87% , 热效应仍然较强, 温度较高, 去除深度较大, 但不会发生明显的燃烧。

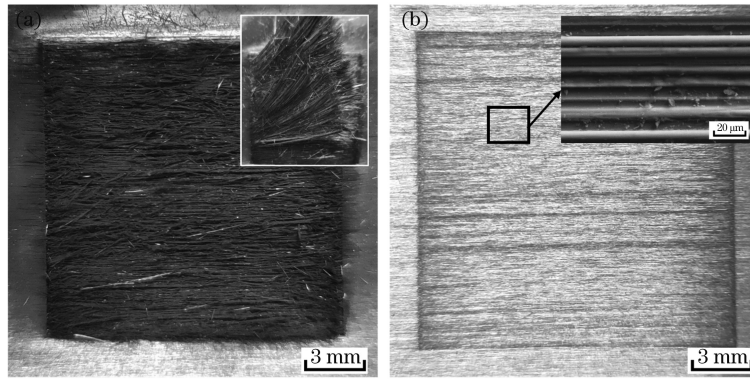


图 6 低扫描速度下 CFRP 的表面形貌。(a) 100 mm/s;(b) 400 mm/s

Fig. 6 Surface topographies of CFRP at low scanning speed. (a) 100 mm/s; (b) 400 mm/s

根据 C 组参数测试扫描速度与光斑搭接率对去除深度和去除效率的影响规律,如图 7 所示。随着扫描速度的增大,脉冲间的预热作用迅速减弱,温度降低,去除深度迅速减小。速度大于 800 mm/s 后,速度的影响减弱,去除深度的变化较小,因此去

除效率随扫描速度的加快而显著提高。扫描速度为 2600~4000 mm/s 时,去除深度和效率并不是随扫描速度的提高单调减小,而是在 3200 mm/s 的速度处出现一个峰值,该速度下相邻脉冲间隔为 64 μm,此时光斑搭接率接近 0。图 8 为该扫描速度下两个

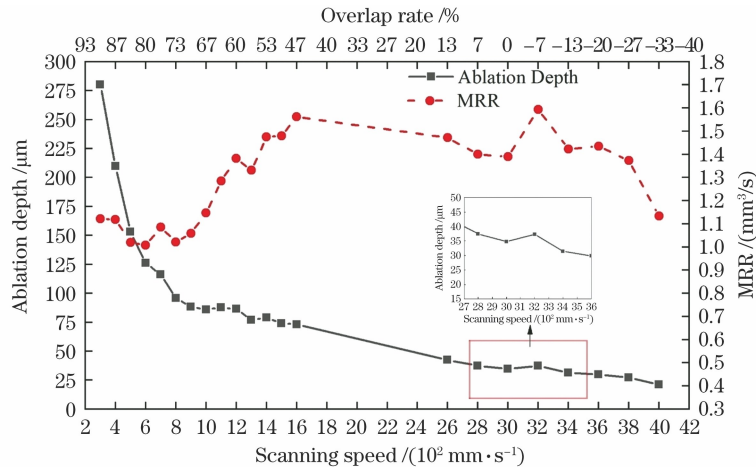


图 7 扫描速度对去除深度和去除效率的影响规律

Fig. 7 Influences of scanning speed on ablation depth and MRR

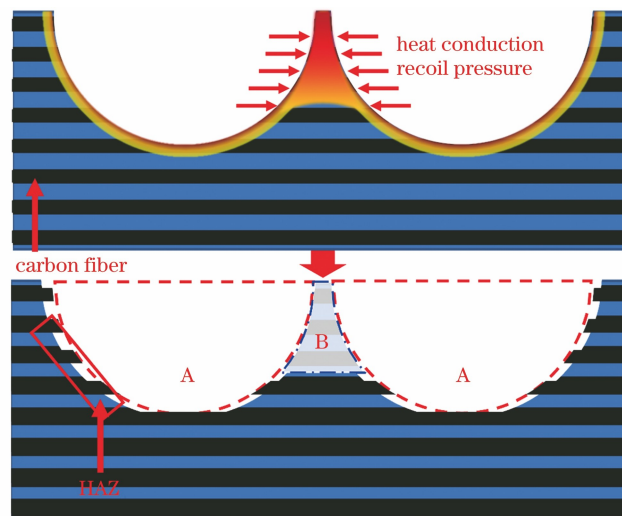


图 8 热-机械剥蚀作用下表面材料去除示意图

Fig. 8 Schematic of surface material removal under thermo-mechanical ablation

相邻激光脉冲作用瞬间的温度场分布和材料去除机制示意图,当光斑未搭接且接近搭接状态时,激光直接作用区域的功率密度足够高,能够直接烧蚀气化碳纤维,即图 8 中的 A 区域。两个光斑之间未被激光直接作用的 B 区域中的 CFRP 在热传导的作用下被加热,部分树脂被烧蚀气化,残留的松散碳纤维在树脂和碳纤维气化反冲压力作用下被去除,在这种热-机械剥蚀的作用下去除效率最高。

图 9 为根据 D 组参数测试的填充间距和光斑搭接率 α_B 对去除深度和去除效率的影响规律。在 30~50 μm 的填充间距时,去除深度随填充间距的增大迅速减小。如图 9(a)、(b)所示,在填充间距达到 150~160 μm 时,去除效率出现峰值。分析其物理过程,如图 10 所示,相较于相邻脉冲之间的热扩散,扫描路径上的激光作用向相邻扫描路径的热扩

散时间较长,热扩散距离更大,更大范围 CFRP 在热扩散作用下被预热,部分树脂被烧蚀气化,残留的松散碳纤维在树脂气化反冲压力作用下被去除。

如图 9 所示,在 30~90 μm 的填充间距下,光斑搭接率 α_B 为 70%~10%, 0° 平行扫描下的去除效率更高,而在 90~180 μm 的填充间距下,光斑搭接率 α_B 为 10%~ -80%, 90° 垂直扫描下的去除效率更高。在 30~90 μm 的填充间距条件下,沿扫描路径和垂直于扫描路径的光斑搭接紧密,热效应起主要作用, 0° 平行扫描下的预热作用强,温度高,去除效率高。在大填充间距条件下, 0° 平行扫描下相邻两条扫描路径没有搭接,如图 10(a)所示; 90° 垂直扫描如图 10(b)所示,碳纤维较高的轴向热导率导致扫描路径间的 CFRP 热扩散更充分,去除效率更高。

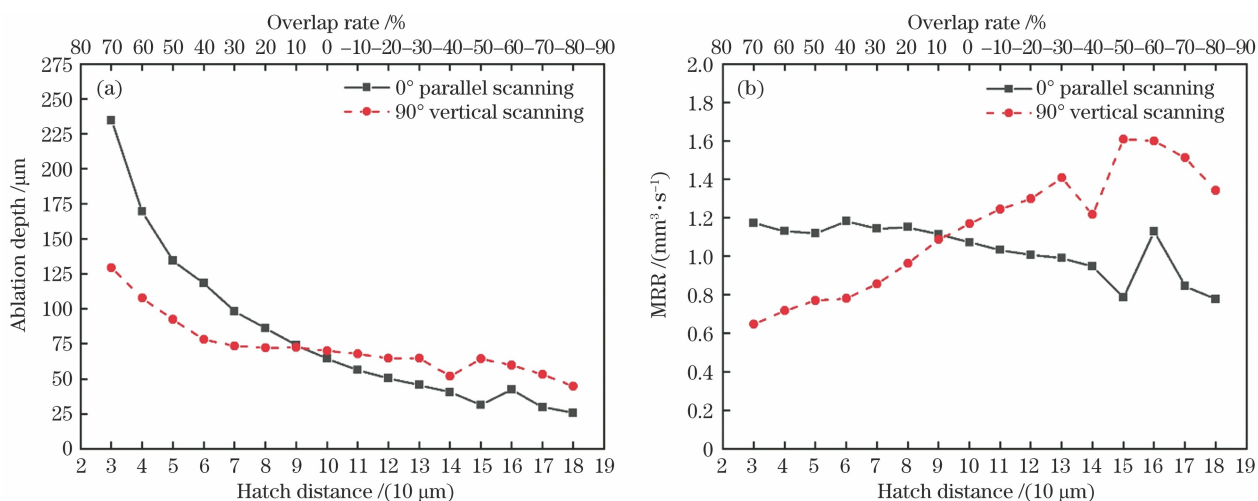


图 9 0° 和 90° 扫描下填充间距对去除深度和效率的影响。(a) 去除深度;(b) 去除效率

Fig. 9 Influences of hatch distance on ablation depth and MRR at 0° and 90° scanning angles. (a) Ablation depth; (b) MRR

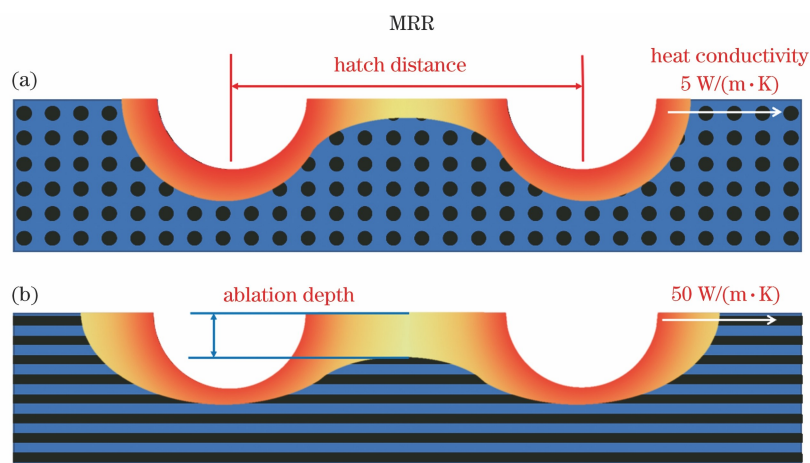


图 10 扫描轨迹上多个脉冲作用后的热扩散示意图。(a) 0° 扫描;(b) 90° 扫描

Fig. 10 Schematics of thermal diffusion after multiple pulses on scanning path. (a) 0° parallel scanning; (b) 90° vertical scanning

3.4 多层阶梯形去除

对于阶梯形的去除挖补加工,随着去除层数的增加,加工表面逐渐远离焦平面,因此需要结合场镜的聚焦深度来考虑是否需要实时调整加工系统与样品表面的距离。如图 11 所示,在 ZT7H/QY9611 碳纤维复合层板上进行多层阶梯形去除,每层厚度为 $125\ \mu\text{m}$,去除区域直径为 $90\ \text{mm}$,去除角度为 3.6° ,去除层数为 18,总去除深度约为 $2.2\ \text{mm}$ 。采用 E 组参数扫描两次去除一层碳纤维,然后调整扫描路径以保持扫描角度为 0° ,去除过程中固定激光加工头与样品的相对位置,因此多层去除是一个逐渐离焦的过程。图 12(a)、(b)分别为轮廓仪通过线扫描测得的图 11 中 AB 和 CD 截面的表面轮廓,经过计算后得到图 13 所示的去除深度与离焦距离之间的关系图,数据拟合后整体呈现去除深度随离焦距离的增大而减小的趋势,由于该激光系统聚焦光

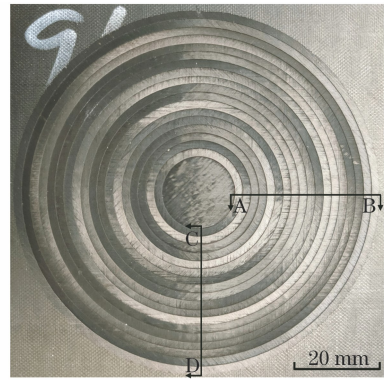


图 11 多层去除后 CFRP 表面的宏观形貌
Fig. 11 Surface morphology of CFRP after multi-layer removal

束的瑞利长度约为 $2.7\ \text{mm}$,多层去除过程中样品始终处于瑞利长度范围内,因此去除深度的精度控制为 $\pm 20\ \mu\text{m}$ 。

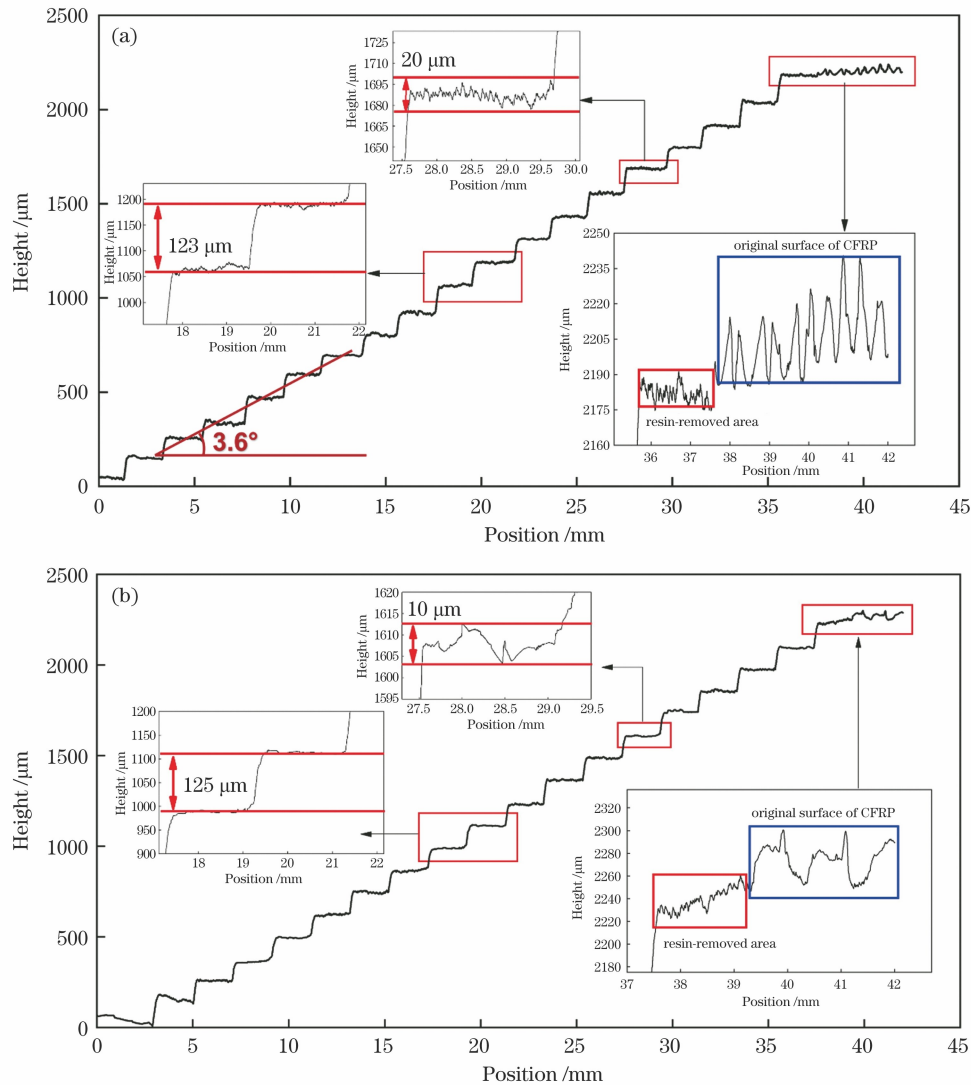


图 12 图 11 中 AB 和 CD 截面的表面轮廓。(a) AB; (b) CD

Fig. 12 Surface profiles of AB and CD sections in Fig. 11. (a) AB; (b) CD

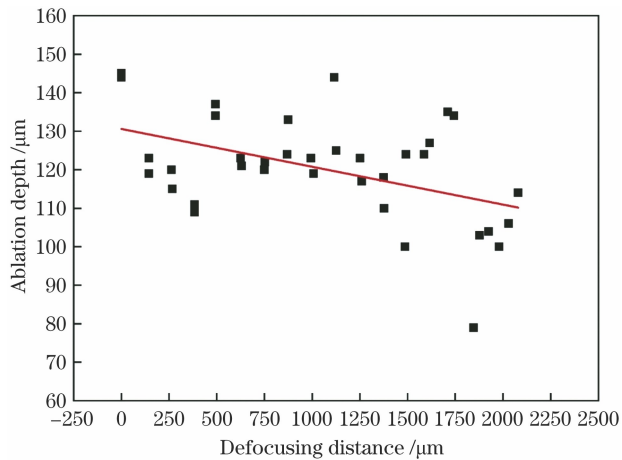


图 13 多层去除时离焦距离对去除深度的影响

Fig. 13 Influence of defocusing distance on ablation depth during multi-layer removal

4 结 论

研究了 1064 nm 纳秒脉冲激光进行 CFRP 去除挖补加工时,峰值功率密度、扫描角度以及光斑搭接率等工艺参数对去除效率和去除质量的影响规律以及其中的物理机制。基于各向异性传热机理研究了激光扫描角度对材料去除率的影响规律,扫描角度越大,预热效应越弱,去除效率越低且去除质量越差。探索了光斑搭接率对非匀质材料热-机械剥蚀影响的规律与物理机制,利用该机制可以提高去除效率。进行了 CFRP 多向层板的 18 层阶梯形去除,精度控制在 $\pm 20 \mu\text{m}$,同时讨论了激光离焦状态对去除效果的影响。对工艺参数影响规律的研究能够为实际加工应用提供工艺优化策略,提高加工效率和质量。关于多工艺参数的共同影响规律及其微观物理机制的研究有待后续开展。

参 考 文 献

- [1] 杜善义, 关志东. 我国大型客机先进复合材料技术应对策略思考[J]. 复合材料学报, 2008, 25(1): 1-10. Du S Y, Guan Z D. Strategic considerations for development of advanced composite technology for large commercial aircraft in China[J]. Acta Materiae Compositae Sinica, 2008, 25(1): 1-10.
- [2] Moutier J, Fois M, Picard C. Characterization of carbon/epoxy materials for structural repair of carbon/BMI structures [J]. Composites Part B: Engineering, 2009, 40(1): 1-6.
- [3] Zhang G X, Hua X M, Huang Y, et al. Investigation on mechanism of oxide removal and plasma behavior during laser cleaning on aluminum alloy[J]. Applied Surface Science, 2020, 506: 144666.
- [4] 胡登文, 刘艳, 陈辉, 等. Q960E 钢激光熔覆 Ni 基 WC 涂层组织及性能[J]. 中国激光, 2021, 48(6): 0602120. Hu D W, Liu Y, Chen H, et al. Microstructure and properties of laser cladding Ni-based WC coating on Q960E steel[J]. Chinese Journal of Lasers, 2021, 48(6): 0602120.
- [5] Li W Y, Zhang G J, Huang Y, et al. UV laser high-quality drilling of CFRP plate with a new interlaced scanning mode [J]. Composite Structures, 2021, 273: 114258.
- [6] Leone C, Genna S. Heat affected zone extension in pulsed Nd:YAG laser cutting of CFRP[J]. Composites Part B: Engineering, 2018, 140: 174-182.
- [7] Leone C, Mingione E, Genna S. Laser cutting of CFRP by quasi-continuous wave (QCW) fibre laser: effect of process parameters and analysis of the HAZ index[J]. Composites Part B: Engineering, 2021, 224: 109146.
- [8] 梅欢欢, 崔健磊, 程杨, 等. 飞秒激光诱导多壁碳纳米管与金属电极连接的实验研究[J]. 中国激光, 2021, 48(8): 0802019. Mei H H, Cui J L, Cheng Y, et al. Experimental study on connection between multiwalled carbon nanotubes and metal electrodes under femtosecond laser irradiation[J]. Chinese Journal of Lasers, 2021, 48(8): 0802019.
- [9] 翟兆阳, 梅雪松, 王文君, 等. 碳化硅陶瓷基复合材料激光刻蚀技术研究进展[J]. 中国激光, 2020, 47(6): 0600002. Zhai Z Y, Mei X S, Wang W J, et al. Research advancement on laser etching technology of silicon carbide ceramic matrix composite [J]. Chinese Journal of Lasers, 2020, 47(6): 0600002.
- [10] Fujita M, Ohkawa H, Somekawa T, et al. Wavelength and pulsewidth dependences of laser processing of CFRP[J]. Physics Procedia, 2016, 83: 1031-1036.
- [11] Bluemel S, Jaeschke P, Suttman O, et al. Comparative study of achievable quality cutting carbon fibre reinforced thermoplastics using continuous wave and pulsed laser sources[J]. Physics Procedia, 2014, 56: 1143-1152.
- [12] Sato Y, Tsukamoto M, Nariyama T, et al. Experimental study of CFRP cutting with nanosecond lasers[J]. Transactions of JWRI, 2013, 42(1): 23-26.
- [13] Wolynski A, Herrmann T, Mucha P, et al. Laser ablation of CFRP using picosecond laser pulses at different wavelengths from UV to IR [J]. Physics Procedia, 2011, 12: 292-301.
- [14] Fischer F, Romoli L, Kling R. Laser-based repair of

- carbon fiber reinforced plastics [J]. *CIRP Annals*, 2010, 59(1): 203-206.
- [15] Schmutzler H, Popp J, Büchter E, et al. Improvement of bonding strength of scarf-bonded carbon fibre/epoxy laminates by Nd:YAG laser surface activation [J]. *Composites Part A: Applied Science and Manufacturing*, 2014, 67: 123-130.
- [16] Genna S, Leone C, Ucciardello N, et al. Increasing adhesive bonding of carbon fiber reinforced thermoplastic matrix by laser surface treatment [J]. *Polymer Engineering & Science*, 2017, 57(7): 685-692.
- [17] Leone C, Genna S. Effects of surface laser treatment on direct co-bonding strength of CFRP laminates [J]. *Composite Structures*, 2018, 194: 240-251.
- [18] Hu J, Xu H B. Pocket milling of carbon fiber-reinforced plastics using 532-nm nanosecond pulsed laser: an experimental investigation [J]. *Journal of Composite Materials*, 2016, 50(20): 2861-2869.
- [19] Genna S, Tagliaferri F, Papa I, et al. Multi-response optimization of CFRP laser milling process based on response surface methodology [J]. *Polymer Engineering & Science*, 2017, 57(6): 595-605.
- [20] Leone C, Papa I, Tagliaferri F, et al. Investigation of CFRP laser milling using a 30 W Q-switched Yb:YAG fiber laser: effect of process parameters on removal mechanisms and HAZ formation [J]. *Composites Part A: Applied Science and Manufacturing*, 2013, 55: 129-142.
- [21] Loutas T H, Sotiriadis G, Tsonos E, et al. Investigation of a pulsed laser ablation process for bonded repair purposes of CFRP composites via peel testing and a design-of-experiments approach [J]. *International Journal of Adhesion and Adhesives*, 2019, 95: 102407.
- [22] Loutas T H, Sotiriadis G, Bonas D, et al. A statistical optimization of a green laser-assisted ablation process towards automatic bonded repairs of CFRP composites [J]. *Polymer Composites*, 2019, 40(8): 3084-3100.
- [23] Holder D, Buser M, Boley S, et al. Image processing based detection of the fibre orientation during depth-controlled laser ablation of CFRP monitored by optical coherence tomography [J]. *Materials & Design*, 2021, 203: 109567.
- [24] Ledesma R I, Palmieri F L, Lin Y, et al. Picosecond laser surface treatment and analysis of thermoplastic composites for structural adhesive bonding [J]. *Composites Part B: Engineering*, 2020, 191: 107939.
- [25] Xu H B, Hu J. Modeling of the material removal and heat affected zone formation in CFRP short pulsed laser processing [J]. *Applied Mathematical Modelling*, 2017, 46: 354-364.
- [26] 吴恩启, 石玉芳, 李美华, 等. 编织碳纤维复合材料平面内热传导规律研究 [J]. *中国激光*, 2016, 43(7): 0703004.
- Wu E Q, Shi Y F, Li M H, et al. In-plane thermal conduction of woven carbon fiber reinforced polymers [J]. *Chinese Journal of Lasers*, 2016, 43(7): 0703004.

Mechanism of Laser Thermo-Mechanical Ablation of Carbon Fiber Composites

Liang Han^{1,2,3}, Zhao Shusen^{1,3*}, Jiang Lu^{1,2,3}, Zou Chen¹, Xu Jie¹,
Zhang Zhiyan^{1,3}, Lin Xuechun^{1,2,3}

¹Laboratory of All-Solid-State Light Sources, Institute of Semiconductors, Chinese Academy of Sciences, Beijing 100083, China;

²College of Materials Science and Opto-Electronic Technology, University of Chinese Academy of Sciences, Beijing 100049, China;

³Engineering Technology Research Center of All-Solid-State Lasers Advanced Manufacturing, Beijing 100083, China

Abstract

Objective Carbon fiber reinforced plastics (CFRP) are widely used in aerospace, sports, medical, transportation and other fields due to their advantages of high specific strength and high specific modulus. Taking Boeing 787 aircraft as an example, the mass fraction of composites in the aircraft structure has reached more than 50%. Composite structures of the aircraft are vulnerable to be damaged in harsh environments during long-term service, and composite structure repairing is an important part in aviation equipment maintenance. The committed step of

composite structure repairing is the damaged zone removal at a small angle, usually 2° – 6° , which is difficult for mechanical processing. At present, it mainly relies on manual grinding, which shows low efficiency and poor controllability. Laser beam machining (LBM) has the advantages of high precision, high efficiency, and high controllability. It is suitable for difficult-to-machine materials including CFRP, and has excellent performance in laser cutting, drilling, welding, cleaning, etching and other applications. The structural characteristics and thermal-physical properties of CFRP materials result in a more complex physical process for laser removal of CFRP than that for metal materials. The existing studies mainly focus on the thermal process of laser removal of CFRP and the surface state evolution mechanism, but little attention is paid to the thermal-mechanical couple ablation process based on the non-homogeneous characteristics of the CFRP. In this paper, a 1064 nm nanosecond pulsed laser is used for laser removal of CFRP, and the effects of process parameters on removal efficiency, quality as well as the process optimization methods are studied. Based on the anisotropic heat transfer mechanism, the effect of laser scanning angle on material removal rate (MRR) is investigated and the influence of laser spot overlapping rate on thermal-mechanical ablation of CFRP is also discussed.

Methods Multidirectional and unidirectional carbon fiber composite laminates are milled by a 1064 nm nanosecond laser. Fig. 1 shows the laser scanning area and path. The solid line represents the light-on state, and the dashed line represents the light-off state. The variations of ablation depth (h) with power (P), scanning speed (v), hatching distance (d), and scanning angle (θ) are tested, and the variations of the corresponding MRR with process parameters are also calculated. The macroscopic and microscopic morphologies of the sample surfaces are obtained by optical microscope and scanning electron microscope.

Results and Discussions The laser peak power density shows a significant effect on the removal quality. Since the transmittance of the epoxy resin matrix in CFRP to the 1064 nm wavelength laser is about 80%, most of the laser penetrates the surface resin and directly acts on the carbon fiber during laser processing of CFRP, causing the carbon fiber to heat up, oxidize, and vaporize. Under the action of heat conduction, the epoxy resin around the carbon fiber is heated, ablated, and vaporized. The surface morphologies under different peak power densities are shown in Fig. 3. Since the axial thermal conductivity of the carbon fiber is about ten times the radial thermal conductivity, the preheating effect is more significant when the scanning direction is along the carbon fiber axial direction which results in a decrease in MRR with the increase of scanning angle (Fig. 4). The scanning speed and hatching distance determine the spot overlapping rate (α_A) along the scanning direction and the spot overlapping rate (α_B) perpendicular to the scanning path, respectively. As shown in Figs. 7 and 9, at a specific overlapping rate, the MRR peaks, which is caused by the thermal-mechanical ablation effect (Figs. 8 and 10). Multi-layer stepped removal of multi-directional carbon fiber composite laminates is carried out, and it is found that the ablation depth decreases with the increase of defocusing distance (Fig. 13). When the defocusing distance is shorter than the Rayleigh length of the focused beam, the precision of the removal depth is controlled within $\pm 20 \mu\text{m}$ (Fig. 12).

Conclusions In this paper, the influences of process parameters such as peak power density, scanning angle, and spot overlapping rate on MRR and removal quality are investigated, and the physical mechanism is disclosed in the removal process of CFRP with a 1064 nm nanosecond pulsed laser. Based on the anisotropic heat transfer mechanism, the influence of laser scanning angle on the material removal rate is studied. The smaller the scanning angle, the more significant the preheating effect, and the larger the ablation depth, $220 \mu\text{m}$ at 0° and $150 \mu\text{m}$ at 90° . The physical mechanism of the effect of spot overlapping rate on the thermal-mechanical ablation of non-homogeneous materials is explored, and MRR is improved by using this mechanism. The 18-layer stepped removal of the multi-directional CFRP laminate is carried out, and the precision is controlled within $\pm 20 \mu\text{m}$. The influence of laser defocusing state on MRR is discussed. This research provides a process optimization strategy for practical processing applications and improves the processing efficiency and quality.

Key words laser technique; pulsed laser; carbon fiber composite; scarf repair; thermo-mechanical ablation; multi-layer removal